JOURNAL OF AGRICULTURAL AND FOOD CHEMISTRY

Article

pubs.acs.org/JAFC

High-Resolution Screening Combined with HPLC-HRMS-SPE-NMR for Identification of Potential Health-Promoting Constituents in Sea Aster and Searocket—New Nordic Food Ingredients

Sileshi G. Wubshet,[†] Jeppe S. Schmidt,[†,§,△] Stefanie Wiese,[§,○] and Dan Staerk*[,†,§]

[†]Department of Drug Design and Pharmacology, Faculty of Health and Medical Sciences, University of Copenhagen, Universitetsparken 2, DK-2100 Copenhagen, Denmark

[§]Department of Basic Sciences and Environment, Faculty of Life Sciences, University of Copenhagen, Thorvaldsensvej 40, DK-1870 Frederiksberg C, Denmark

Supporting Information

ABSTRACT: Sea aster (*Aster tripolium* L.) and searocket (*Cakile maritima* Scop.), potential ingredients in the New Nordic Diet, were analyzed by high-resolution radical scavenging and high-resolution α-glucosidase inhibition assays. Results from the two bioactivity profiles were used to guide subsequent structural analysis toward constituents with potential health-promoting effects. Structural analysis was performed by high-performance liquid chromatography–high-resolution mass spectrometry–solid-phase extraction and automated tube transfer nuclear magnetic resonance spectroscopy, that is, HPLC-HRMS-SPE-*tt*NMR. High-resolution mass spectrometry together with detailed analysis of one- and two-dimensional proton detected NMR experiments enabled unambiguous assignment of the targeted analytes. This revealed a series of caffeoyl esters (**1**, **2**, **5**), flavonoid glycosides (**3**, **4**, **6**, **11**–**15**), flavonoids (**7**–**9**), sinapate esters (**10**, **16**, **17**), and sinapinic acid (**18**) associated with radical scavenging and/or α-glucosidase inhibition. In vitro assays implemented in this study showed that sea aster holds potential as a future functional food ingredient for lowering postprandial blood glucose level for diabetics, but further investigations are needed to prove the effect in vivo.

KEYWORDS: *New Nordic Diet, high-resolution screening, HPLC-SPE-tube transfer NMR, α-glucosidase, radical scavenging*

INTRODUCTION

Increased mortality and severe diseases caused by our lifestyle are major threats modern societies have to face in the 21st century. The global status report from the World Health Organization highlighted in 2010 that 36 million of the 57 million deaths that occurred globally in 2008 were due to noncommunicable diseases, including diabetes, cardiovascular diseases, and cancer.[1] One of the main risk factors is unhealthy diet, and WHO suggests promotion of healthy diets as one of the means for reducing risk factors for the above-mentioned diseases.

During the past 20 years the Mediterranean-style diet[2] has become popular in science and society due to its protection against lifestyle diseases. However, this specialized and regionally defined diet is hardly applicable and advisable worldwide, and most countries have their own cultural and regional foods that might be health-promoting.[3] Thus, as part of the development of a new tasty, healthy, and environmentally friendly diet in the Nordic region, Claus Meyer and Rene Redzepi wrote the New Nordic Cuisine manifesto in 2004.[4] The manifest was signed by other leading Nordic chefs later that year and subsequently adopted in the New Nordic Food program by the Nordic Council of Ministers in 2005.[5] The New Nordic Cuisine has become very popular and is currently being developed in interdisciplinary research teams.[6,7] It is rated as a world-class cuisine, exemplified by restaurant NOMA's first place on San Pellegrino's top 50 list of the world's best restaurants from 2010 to 2012.[8] The New Nordic Diet is based on an increased consumption of locally produced fruits, vegetables, herbs, whole grains, seafood, and less but better meat and includes the use of wild plants from the Nordic region. It has recently been shown that a diet based on Nordic food with expected health-promoting effects, for example, berries, cabbages, apples, pears, root vegetables, legumes, oats, rye, and fish, is related to lower mortality and might be effective for lowering weight and hypercholesterolemia.[9,10] Many of the above-mentioned plant-based ingredients contain phytonutrients such as polyphenols, carotenoids, polyunsaturated fatty acids, and plant sterols, which have been shown to exhibit potential health-promoting effects based on in vitro and animal studies.[11−13] However, the potential health-promoting effect of wild-grown plants used in the New Nordic Diet is hardly understood due to incomplete knowledge of their chemical composition and the biochemical properties of individual phytochemicals.

Most investigations of chemical and biological properties of plant-based food are based on either (i) measurement of the biochemical activity of the combined pool of compounds in complex extracts or (ii) bioassay-guided fractionation, which suffers from loss of resolution in the fractionation process and thus limits findings to the most abundant constituents.

Received: July 7, 2013
Revised: August 19, 2013
Accepted: August 20, 2013
Published: August 20, 2013

   dx.doi.org/10.1021/jf402949y | J. Agric. Food Chem. 2013, 61, 8616−8623

However, a new analytical technology platform holds promise for improved profiling of individual bioactive compounds in complex mixtures. The first component of the platform is high-resolution screening or high-resolution bioassay,[14−17] a screening technology that combines microplate-based biochemical detection with the resolution power of analytical-scale high-performance liquid chromatography. The second component is a state-of-the-art hyphenated system consisting of high-performance liquid chromatography, solid-phase extraction, and nuclear magnetic resonance, that is, HPLC-SPE-NMR,[18,19] which has proven to be successful for fast and efficient analysis of the chemical composition of pharmaceuticals[20] and plant extracts,[21−24] including the combined use with circular dichroism to establish absolute configuration of identified metabolites.[25] However, stand-alone HPLC-SPE-NMR analysis does not give any information about the bioactivity of the individual constituents, and for this reason the recent combination with high-resolution screening assays, that is, HR-(bio)assay/HPLC-SPE-NMR,[26−31] is an important new improvement of the basic HPLC-SPE-NMR technique.

Species of the Asteraceae and Brassicaceae family are among the most consumed wild-gathered food in European Mediterranean,[32] and several pharmacological studies have indicated potential health effects of metabolites from these species.[33,34] The present study aims at profiling bioactive compounds in two wild-grown beach plants, as examples of possible food ingredients from Nordic coastal regions, that is, sea aster (*Aster tripolium* L., Asteraceae) and searocket (*Cakile maritima* Scop., Brassicaceae). By means of high-resolution radical scavenging and high-resolution α-glucosidase inhibition assays, individual bioactive compounds in extracts of sea aster and searocket were pin-pointed and subsequently identified using HPLC-HRMS-SPE-*tt*NMR (*tt*NMR, tube-transfer NMR).

MATERIALS AND METHODS

Chemicals. 2,2′-Azinobis(3-ethylbenzothiazoline-6-sulfonic acid) diammonium salt (ABTS), α-glucosidase (type I, from baker's yeast), *p*-nitrophenolglucopyranoside (PNPG), sodium phosphate dibasic dihydrate, methanol-d_3 (99.80% D, HDO + D_2O < 0.03%), and sodium phosphate monobasic dihydrate were purchased from Sigma-Aldrich (St. Louis, MO, USA). Solvents were of analytical or HPLC grade (Sigma-Aldrich), and water was purified by deionization and 0.22 μm membrane filtration (Millipore, Billerica, MA, USA). Formic acid was purchased from Merck (Darmstadt, Germany).

Plant Material and Extraction. Sea aster (*A. tripolium*) and searocket (*C. maritima*) were collected on a sandy beach at Amager (N 55° 33.731′, E 12° 33.704′, 0 m elevation), Copenhagen, Denmark, in October 2011. Searocket was rinsed with distilled water to remove salt and sand, dried, and pulverized in a coffee grinder. Voucher specimens of sea aster and searocket (KU-DS14 and KU-DS15, respectively) have been deposited in Herbarium C (Botanical Museum, University of Copenhagen, Copenhagen, Denmark). Ground material of sea aster and searocket were extracted using 70% aqueous methanol. To inactivate plant enzymes, the suspension was boiled for 10 min and subsequently homogenized using a T25 Basic Ultra Turrax (IKA Labortechnik, Stauden, Germany). Extraction was performed for 96 h, and the extraction solvent was removed under reduced pressure at temperatures below 40 °C. This afforded 8.33 g extract/100 g of sea asters and 3.09 g extract/100 g of searocket.

High-Resolution Radical Scavenging Assay. Chromatographic separation of raw extracts was performed with an Agilent 1200 series instrument (Santa Clara, CA, USA) consisting of a G1311A quaternary pump, a G1322A degasser, a G1316A thermostated column compartment, a G1315C photodiode array detector, a G1367C high-performance autosampler, and a G1364C fraction collector, all controlled by Agilent ChemStation ver. B.03.02 software. The column used was a reversed phase Luna $C_{18}(2)$ (Phenomenex, 150 × 4.6 mm, 3 μm, 100 Å) maintained at 40 °C. The aqueous eluent (A) consisted of water/methanol (95:5, v/v), and the organic eluent (B) consisted of methanol/water (95:5, v/v), both acidified with 0.1% formic acid. The eluent flow rate was maintained at 0.8 mL/min with the following elution profile: 0 min, 30% B; 15 min, 45% B; 25 min, 75% B; 35 min, 100% B; 40 min, 100% B; 42 min, 0% B; and 8 min of equilibration. Samples of searocket and sea aster were prepared at concentrations of 250 mg/mL, and separation was performed after a single injection loading of 5 μL. The column out flow was directed to an automated fraction collector, and the eluate from 4 to 28 min was fractionated into two 96-well microplates (resolution = 8 points per min) (Sterilin Limited, Aberbargoed Caerphilly, UK). The microplate-based radical scavenging assay was based on the procedure described by Re et al.[35] and modified for use in high-resolution microplate assays.[29,31] In short, $ABTS^{\bullet+}$ stock solution was prepared by incubating ABTS (2.5 mM) with 0.875 mM potassium persulfate in Milli-Q water and allowing the mixture to stand in the dark for 12−16 h before use. The $ABTS^{\bullet+}$ working solution was prepared by 5-fold dilution of the stock solution with 0.1 M sodium phosphate buffer (pH 7.4), and 200 μL of this working solution was added to each well. Spectrophotometric measurements of absorbance at 620 nm were performed each minute for 20 min using a Thermo Scientific Multiskan FC microplate photometer (Thermo Scientific, Waltham, MA, USA) controlled by SkanIt ver. 2.5.1 software. $ABTS^{\bullet+}$ reduction values for each well were plotted at its respective retention time as a radical scavenging profile underneath the HPLC chromatogram.

High-Resolution Microplate-Based α-Glucosidase Inhibition Assay. Chromatographic separation of sea aster and searocket was performed as described above, using 10 μL injections of 250 mg/mL extracts. The eluate from 4 to 28 min was fractionated into two 96-well microplates (resolution = 8 points per min) and subsequently evaporated to dryness using an SPD121P Savant SpeedVac concentrator (Thermo Scientific) equipped with an OFP400 oil free pump and a RVT400 refrigerated vapor trap. The α-glucosidase inhibition assay was performed in 0.1 M sodium phosphate buffer (pH 7.5) containing 0.02% sodium azide. The buffer was used for preparing a 10 mM PNPG solution and a 0.1 unit/mL solution of α-glucosidase. Residues in each well were dissolved in 10 μL of dimethyl sulfoxide, and 70 μL of buffer and 100 μL of α-glucosidase solution were added. Well plates were incubated at 28 °C for 10 min before addition of 20 μL of PNPG solution. The formation of *p*-nitrophenol by α-glucosidase was monitored at 405 nm for 35 min, and absorption values (after 20 min reaction time) for each well were plotted at its respective retention time as an inhibition profile underneath the HPLC chromatogram.

HPLC-HRMS-SPE-*tt*NMR Analysis. Chromatographic separations were performed using an Agilent 1100 system (Santa Clara, CA, USA) comprising a G1315A photodiode array detector, a G1313A autosampler, a G1311A quaternary pump, a G1322A degasser, and a G1316A thermostated column compartment. Chromatographic conditions (column, solvent composition, temperature, gradient profile) were the same as described above. A small proportion (0.1%) of the HPLC eluate was directed to a micrOTOF-Q II mass spectrometer (Bruker Daltonik GmbH, Bremen, Germany) equipped with an electrospray ionization interface. Mass spectra were acquired in positive-ion mode, using a drying temperature of 200 °C, a capillary voltage of 4100 V, a nebulizer pressure of 2.0 bar, and a drying gas flow of 7 L/min. A solution of sodium formate clusters was automatically injected in the beginning of each run to enable internal mass calibration. The rest of the HPLC eluate was directed to the photodiode array detector and subsequently to a Prospekt 2 SPE-unit (Spark Holland, Emmen, The Netherlands). Cumulative SPE trappings of individual analytes were performed for 10 consecutive injections (30 μL/injection), using either absorption thresholds (254, 280, 310, and 360 nm) or mass count thresholds (from base peak chromatograms) to trigger analyte trapping. Chromatography, peak trapping, and analyte transfer from the SPE unit were controlled with HyStar ver. 3.2 software (Bruker Biospin GmbH, Rheinstetten, Germany). The HPLC eluate was diluted with Milli-Q water at a

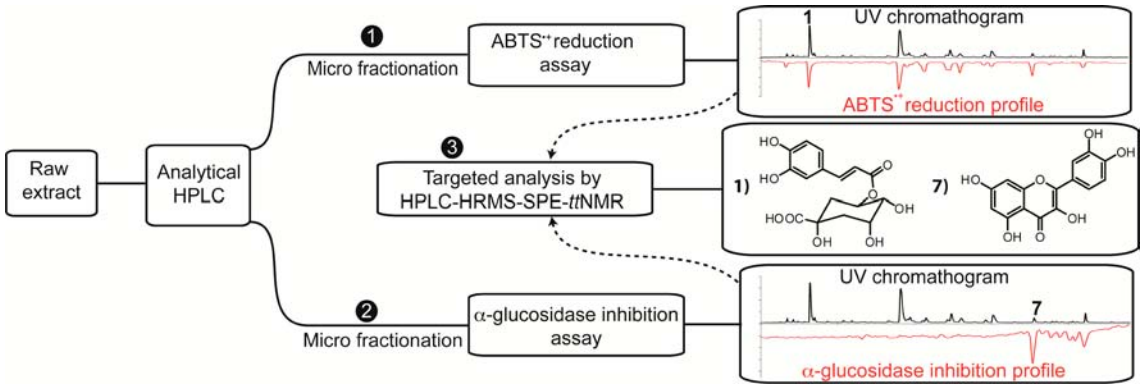

Figure 1. Schematic representation of HPLC-HRMS-SPE-*tt*NMR analysis of sea aster and searocket extract guided by high-resolution ABTS$^{\bullet+}$ reduction and α-glucosidase inhibition profiles. Path 1: microfractionation into two 96-well microplates followed by ABTS$^{\bullet+}$ reduction assay of each microfraction to produce high-resolution ABTS$^{\bullet+}$ reduction profile. Path 2: microfractionation into two 96-well microplates followed by α-glucosidase inhibition assay to produce high-resolution α-glucosidase inhibition profile. Path 3: HPLC-HRMS-SPE-*tt*NMR analysis targeting antioxidants and α-glucosidase inhibitory metabolites established in the preceding procedures.

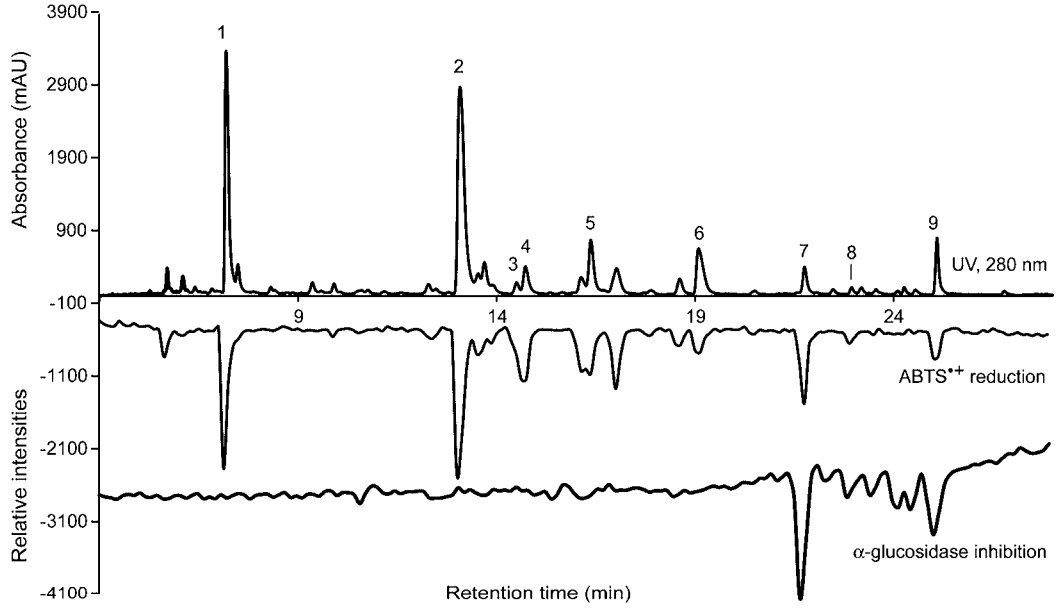

Figure 2. High-resolution α-glucosidase inhibition and radical scavenging profiles of sea aster with overlaid HPLC chromatogram at 280 nm. Peaks are numbered sequentially with increasing elution order.

flow rate of 1.5 mL/min prior to trapping on 10 × 2 mm i.d. Resin GP (general purpose, 5−15 μm, spherical shape, polydivinyl-benzene phase) SPE cartridges from Spark Holland. SPE cartridges were conditioned with 1000 μL of methanol at 6 mL/min and equilibrated with 500 μL of Milli-Q water at 1 mL/min prior to trapping. Loaded cartridges were dried with pressurized nitrogen gas for 45 min each, and the analytes were automatically eluted into 1.7 mm o.d. NMR tubes (96-position tube racks) using a Gilson Liquid Handler controlled by PrepGilson software version 1.2 (Bruker Biospin GmbH).

NMR Experiments. NMR experiments were performed with a Bruker Avance III system (^{1}H operating frequency of 600.13 MHz) equipped with a Bruker SampleJet sample changer and a cryogenically cooled gradient inverse triple-resonance 1.7 mm TCI probe-head (Bruker Biospin) optimized for ^{1}H and ^{13}C observation. Bruker standard pulse sequences were used throughout this study. IconNMR (version 4.2, Bruker Biospin) was used for controlling automated acquisition of NMR data (temperature equilibration to 300 K, optimization of lock parameters, gradient shimming, and setting of receiver gain), and processing of NMR data was performed using Topspin (version 3.0, Bruker Biospin). One-dimensional ^{1}H NMR spectra were acquired using 30° pulses and 64K data points, which were zero-filled to 128K and multiplied with an exponential function (line-broadening = 0.3 Hz) prior to Fourier transformation. Two-dimensional homo- and heteronuclear experiments were acquired with 2048 data points in the direct dimension and 512 (DQF-COSY), 256 (multiplicity-edited HSQC), and 128 (H2BC, HMBC, and ROESY) in the indirect dimension with spectral widths determined from the corresponding one-dimensional experiments. The HMBC and HSQC experiments were optimized for $^nJ_{H,C}$ = 8 Hz and $^1J_{H,C}$ = 145 Hz, respectively. All two-dimensional experiments were processed to 2K × 1K data matrices after application of a sine-bell squared window function in F1 and F2.

RESULTS AND DISCUSSION

Sea aster (*A. tripolium*) and searocket (*C. maritima*) were collected locally in the Copenhagen area in October 2011, and each plant was extracted in 70% boiling methanol immediately after collection to avoid enzymatic degradation of secondary metabolites. Reconstituted samples were subjected to high-resolution radical scavenging and α-glucosidase inhibition

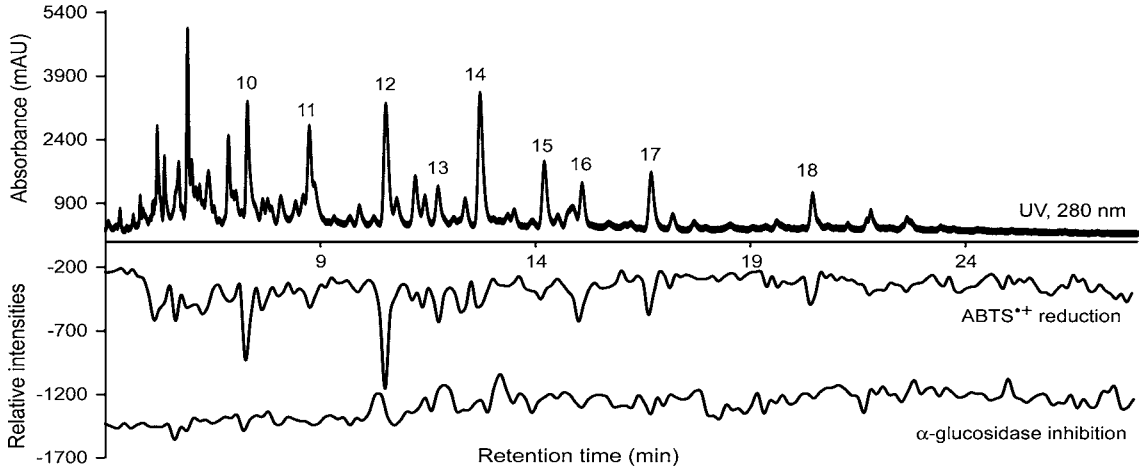

Figure 3. High-resolution α-glucosidase inhibition and radical scavenging profiles of searocket with overlaid HPLC chromatogram at 280 nm. Peaks are numbered sequentially (starting from 10) with increasing elution order.

assays to acquire high-resolution bioactivity profiles used for targeting subsequent HPLC-HRMS-SPE-*tt*NMR analysis toward bioactive constituents only (as depicted schematically in Figure 1).

High-Resolution Bioactivity Profiling. High-resolution radical scavenging and α-glucosidase inhibition profiles of sea aster and searocket are shown underneath their corresponding HPLC chromatograms in Figures 2 and 3, respectively. The radical scavenging profiles show that especially sea aster is rich in discrete and well-separated peaks correlated with radical scavenging activity (Figure 2, peaks 1−9, t_R 7−26 min). Contrary to this, searocket contains only two discrete peaks with strong responses in the high-resolution radical scavenging profile (Figure 3, peaks 10 and 12), in addition to several minor constituents with lower and less well-defined profiles (t_R 4−17 min). For sea aster, two well-defined peaks showing pronounced α-glucosidase inhibitory activity are observed at 20.7 and 24.6 min (Figure 2, peaks 7 and 9). In addition, a range of analytes with very weak responses in the HPLC chromatogram (t_R 21−24 min) are correlated with relatively strong responses in the high-resolution α-glucosidase inhibition profile. This is in contrast to sea rocket (Figure 3), for which no well-defined peaks with α-glucosidase inhibitory activity are observed. The radical scavenging and α-glucosidase inhibition profiles provide good resolution that allows disclosure of the individual metabolites responsible for the observed activities, that is, correlating peaks in the biochromatograms with individual peaks in the overlaid HPLC chromatograms. This information was used for targeting subsequent HPLC-HRMS-SPE-*tt*NMR analysis toward potential bioactive constituents.

HPLC-HRMS-SPE-*tt*NMR. Sea aster (*A. tripolium*) and searocket (*C. maritima*) were subjected to HPLC-HRMS-SPE-*tt*NMR analysis targeted toward those constituents having discrete, well-separated peaks and displaying highest activity in the radical scavenging and/or α-glucosidase inhibition profiles. The HPLC peaks were numbered 1−9 and 10−18 in order of increasing retention time from each plant (Figures 2 and 3, respectively), and the identified metabolites were numbered **1**−**9** and **10**−**18** accordingly. Results from NMR and LC-HRMS analyses (Tables S1 and S2 in the Supporting Information) led to the identification of caffeoyl esters, flavonoids, flavonoid glycosides, sinapate esters, and sinapinic acid in the two plants.

Caffeoyl Esters. Sea aster contained three caffeoyl esters, **1**, **2**, and **5**, displaying discrete peaks with pronounced activity in the radical scavenging profile. Peak 1 showed a M + H ion with m/z 355.1021 corresponding to the molecular formula of $C_{16}H_{18}O_9$ for compound **1**. The ^{1}H NMR spectrum showed characteristic signals of *E*-caffeoyl and quinic acid moieties. The downfield position of H-5 (5.33 ppm) was interpreted as the result of esterification at C-5 of quinic acid; thus, the structure of compound **1** was assigned to 5-*O*-caffeoylquinic acid[36] (Figure 4). On the basis of HRMS, peaks 2 and 5 were identified as isobaric compounds with the molecular formula $C_{25}H_{24}O_{12}$, and the ^{1}H NMR spectra showed that these two compounds contained two *E*-caffeoyl units each and a single quinic acid. For compound **2**, large downfield shifts of H-3 (δ 5.43) and H-5 (δ 5.39) were observed, whereas large downfield shifts of H-4 (δ 5.11) and H-5 (δ 5.43) were observed for **5**. This shows that **2** and **5** are 3,5-*O*-dicaffeoylquinic acid and 4,5-*O*-dicaffeoylquinic acid, respectively. ^{1}H NMR data given in Table S1 of the Supporting Information were in agreement with those reported in the literature.[37]

Flavonoid and Flavonoid Glycosides. Peaks 7−9 showed discrete signals in the radical scavenging profile as well as in the α-glucosidase inhibition profile. On the basis of HRMS analysis, peak 7 was assigned to a molecular formula of $C_{15}H_{10}O_7$, and AMX and AX spin systems observed in the downfield region of the ^{1}H NMR spectrum were in agreement with quercetin (**7**).[33] Peak 8 was assigned the molecular formula $C_{15}H_{10}O_6$ on the basis of HRMS and showed the same multiplicity pattern as quercetin, but with an additional flavone H-3 resonance at 6.55 ppm. This established the structure of compound **8** as luteolin.[38] Peak 9 was assigned the molecular formula $C_{15}H_{10}O_5$ on the basis of the M + H ion at m/z 271.0601, and the ^{1}H NMR spectrum showed a characteristic AA′XX′ spin system (δ 7.86 and 6.94), doublets for two meta-coupled hydrogen (δ 6.47, J = 2.1 Hz, H-8 and δ 6.22, J = 2.1 Hz, H-6), and a singlet resonance (δ 6.60, H-3), which is in agreement with apigenin (**9**).[38] Monoglycosides (**3**, **4**, **6**), diglycosides (**13**, **15**), and triglycosides (**11**, **12**, **14**) of flavonoids were recognized on the basis of neutral loss analysis in HRMS and integration of anomeric resonances from ^{1}H NMR spectra. Interglycan and glycan−aglycone linkages were established on the basis of HMBC correlations. Comparison with reference data from the literature revealed their identities as quercetin 3-

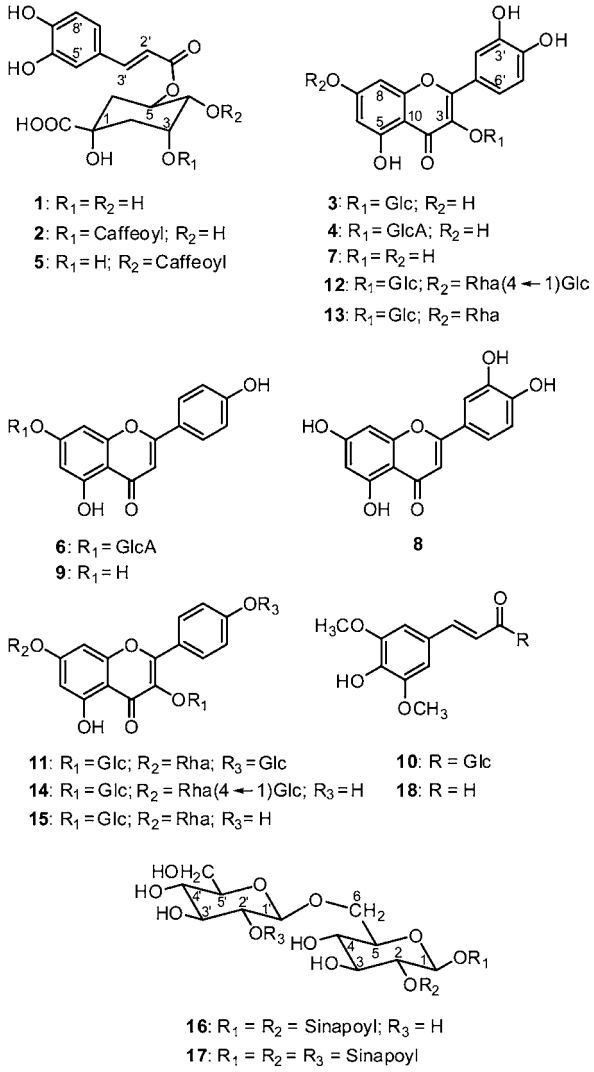

Figure 4. Structures of compounds identified in sea aster (**1**−**9**) and searocket (**10**−**18**).

O-β-D-glucopyranoside (**3**),[36] quercetin 3-*O*-β-D-glucuronide (**4**),[36] apigenin 7-*O*-β-D-glucuronide (**6**),[39] kaempferol 3,4′-di-*O*-β-D-glucopyranoside-7-*O*-α-L-rhamnopyranoside (**11**),[40] quercetin 3-*O*-β-D-glucopyranoside-7-*O*-β-D-glucopyranosyl-(1→4)-α-L-rhamnopyranoside (**12**),[41] quercetin 3-*O*-β-D-glucopyranoside-7-*O*-α-L-rhamnopyranoside (**13**),[41] kaempferol 3-*O*-β-D-glucopyranoside-7-*O*-β-D-glucopyranosyl(1→4)-α-L-rhamnopyranoside (**14**), and kaempferol 3-*O*-β-D-glucopyranoside-7-*O*-α-L-rhamnopyranoside (**15**).[42] Kaempferol 3-*O*-β-D-glucopyranoside-7-*O*-β-D-glucopyranosyl(1→4)-α-L-rhamnopyranoside (**14**) has not previously been reported in the literature. Observed HMBC correlations from anomeric protons H-1″ (Glc) and H-1‴ (Rha) to C-3 and C-7, respectively, are in accordance with 3,7-diglycosylated kaempferol. The connectivity between the two glycans was established on the basis of a strong ^{3}J HMBC correlation from the anomeric proton of the terminal glucose (δ H1′′′′ = 4.63) to a rather deshielded carbon resonance (δ C-4‴ = 82.4) of rhamnose. Similar correlation patterns were observed for compound **12**. Assignment of ^{1}H and ^{13}C resonances for compound **14** is given in Table 1.

Sinapic Acid and Sinapate Esters. Results from HPLC-SPE-HRMS-*tt*NMR analysis revealed four sinapic acid ana-

Table 1. ^{1}H and ^{13}C NMR Data of 14 Acquired in the HPLC-SPE-*tt*NMR Mode

position	^{1}H[a,b,c]	^{13}C[a,c]
aglycone		
2		159.5
3		135.5
4		nd
5		162.7
6	6.48 (1H, d, 2.0)	100.3
7		163.3
8	6.78 (1H, d, 2.0)	95.2
9		157.8
10		107.6
1′		122.8
2′/6′	6.90 (2H, AA′)	115.9
3′/5′	8.09 (2H, XX′)	132.1
4′		161.4
glucose		
1″	5.33 (1H, d, 7.4)	103.4
2″	3.45 (1H, t, 8.9)	75.5
3″	3.42 (1H, t, 9.1)	77.8
4″	3.30* (1H, m)	71.2†
5″	3.21 (1H, m)	78.3
6″	3.52 (1H, dd, 11.9, 5.7)	62.4
	3.69§ (1H, m)	
rhamnose		
1‴	5.56 (1H, br)	99.4
2‴	4.05 (1H, m)	71.4
3‴	4.07 (1H, dd, 9.0, 3.4)	71.9
4‴	3.73 (1H, t, 9.1)	82.4
5‴	3.66 (1H, m)	69.7
6‴	1.33 (1H, d, 6.2)	
glucose		
1′′′′	4.63 (1H, d, 7.9)	105.4
2′′′′	3.22 (1H, dd, 8.9, 8.1)	75.8
3′′′′	3.38 (1H, t, 8.8)	78.0
4′′′′	3.30* (1H, m)	71.2†
5′′′′	3.29 (1H, m)	77.9
6′′′′	3.69§ (1H, m)	62.5
	3.85 (1H, dd, 12.0, 2.1)	

[a] ^{1}H (600 MHz) and ^{13}C (150 MHz) NMR spectroscopic data measured in methanol-d_4; δ values relative to internal TMS. [b] Integrals; multiplicity and coupling constants of signals (given in parentheses): d, doublet; t, triplet; m, multiplet; br, broad; coupling constants (apparent splittings) are reported as numerical values in hertz. [c] Overlapped resonances within the column are flagged with †, *, and §.

logues occurring in searocket. Peak 10 showed three downfield resonances, that is, two resonances corresponding to a trans-disubstituted double bond and one singlet resonance integrating for two hydrogens. Together with another singlet at 3.9 ppm (integrating for six protons), this suggested a symmetrically methoxylated aromatic ring, that is, a 4-hydroxy-3,5-dimethoxycinnamoyl unit. Additional resonances for a glucopyranoside moiety were observed and based on the ^{3}J HMBC correlation from the anomeric proton to the carbonyl carbon at 164.5 ppm. Thus, the structure of compound **10** was concluded to be sinapoyl-*O*-β-D-glucopyranoside.[43] Peaks 16 and 17 showed two and three sets of sinapoyl ^{1}H resonances, respectively, in addition to resonances corresponding to two glucopyranosyl units. This indicated compounds **16** and **17** to be di- and trisinapoyl esters of a disaccharide, and detailed

dx.doi.org/10.1021/jf402949y | J. Agric. Food Chem. 2013, 61, 8616−8623

analysis of 2D NMR experiments concluded the analytes to be 1,2-di-*O*-sinapoyl-*β*-gentiobiose (**16**)[44] and 1,2,2′-tri-*O*-sinapoyl-*β*-gentiobiose (**17**).[41] Peak 18 showed ^{1}H resonances corresponding to the aglycone resonances of peak 10, and thus **18** was identified as sinapic acid.[45]

In conclusion, high-resolution radical scavenging and *α*-glucosidase inhibition profiles of searocket and sea aster showed both plants to be rich in antioxidants, that is, metabolites with radical ($ABTS^{\bullet+}$) scavenging capacity, whereas only sea aster contains a series of metabolites with *α*-glucosidase inhibitory activity. The microplate-based high-resolution bioassays were easy to implement and allowed direct correlation between the peak in the high-resolution bioactivity profile and the corresponding peak in the HPLC chromatogram. Using this information, subsequent HPLC-HRMS-SPE-*tt*NMR analysis was targeted toward bioactive constituents only, thereby focusing labor and costly instrument time toward structure elucidation of the three *α*-glucosidase inhibitors and the18 antioxidants shown in Figure 4. Another advantage of the high-resolution bioassay-guided HPLC-HRMS-SPE-*tt*NMR platform described here is that the relative responses observed in the high-resolution bioassay profiles prevent potential underestimation of highly bioactive constituents due to low abundance and/or low response with the employed detection technique (diode array detector in this case). This is illustrated in the analysis of sea aster, where peak 7 could potentially be underestimated and excluded in a standard HPLC-HRMS-SPE-*tt*NMR analysis due to a relatively low response in the UV trace (Figure 2). However, the *α*-glucosidase inhibition profile disclosed the highest inhibitory response for this constituent, which was therefore included in the HPLC-HRMS-SPE-*tt*NMR analysis.

Possessing phenolic functionality, all identified compounds were expected to have radical ($ABTS^{\bullet+}$) scavenging capacity. This observation is in agreement with the underlying principle of radical reduction via the proton-coupled electron transfer mechanism[46] observed for phenolic compounds.

Despite the widespread distribution of glycosylated polyphenols in the two plants, *α*-glucosidase activity was attributed only to the free aglycones **7**−**9**. The glycosylated analogues **3** and **6** showed no or very low *α*-glucosidase inhibition in vitro compared to their corresponding free aglycones **7** and **9**, which is in agreement with previous findings.[27] Both plants hold potential for increased levels of free aglycones in vivo due to possible bacterial hydrolysis of flavonoid glycosides, that is, **3**, **6**, **12**, and **13**, to their corresponding active aglycones, that is, **7** and **9**. Such hydrolysis of dietary flavonoid glycosides by bacteria from human saliva[47] and intestines[48] has previously been observed, but further studies are needed to investigate whether relevant in vivo concentrations for obtaining a health effect are reached. However, thermal hydrolysis of the flavonoid glycosides via increased cooking temperature can also be suggested as a feasible possibility of transforming the glycosylated metabolites to their corresponding aglycones, thereby increasing their potential health-promoting activity prior to uptake. *α*-Glucosidase inhibition of the three compounds quercetin **7**, luteolin **8**, and apigenin **9** observed in the current study is in agreement with previous findings.[49,50] Especially luteolin (IC_{50} = 0.5−1 mg/mL) was reported to possess stronger inhibition of *α*-glucosidase than the clinically used drug acarbose (IC_{50} = 5 mg/mL).[50]

In summary, sea aster was shown to hold promise as a future functional food ingredient for lowering postprandial blood glucose level for diabetics and avoiding oxidative complications in human biological systems. Searocket was also shown to contain a series of radical scavenging metabolites. However, further investigations are needed to prove the effect in vivo.

■ ASSOCIATED CONTENT

Ⓢ Supporting Information

Tables S1 and S2. This material is available free of charge via the Internet at http://pubs.acs.org.

■ AUTHOR INFORMATION

Corresponding Author

*(D.S.) Phone: +45 3533 6177. Fax: +45 35336001. E-mail: ds@sund.ku.dk.

Funding

S.G.W. was supported by the Drug Research Academy, University of Copenhagen. HPLC equipment used for obtaining high-resolution radical scavenging and *α*-glucosidase profiles was obtained via a grant from The Carlsberg Foundation. The 600 MHz HPLC-HRMS-SPE-NMR system used in this work was acquired through a grant from "Apotekerfonden af 1991", The Carlsberg Foundation, and the Danish Agency for Science, Technology and Innovation via the National Research Infrastructure funds.

Notes

The authors declare no competing financial interest.

△(J.S.S.) Permanent address: LEO Pharma A/S, Industriparken 55, DK-2750 Ballerup, Denmark.

○(S.W.) Permanent address: Chr. Hansen A/S, Bøge Alle 10−12, DK-2970 Hørsholm, Denmark.

■ ABBREVIATIONS USED

ABTS, 2,2′-azinobis(3-ethylbenzothiazoline-6-sulfonic acid) diammonium salt; DQF-COSY, double quantum filtered correlation spectroscopy; H2BC, heteronuclear two-bond correlation; HMBC, heteronuclear multiple-bond correlation; HPLC, high-performance liquid chromatography; HR, high resolution; HRMS, high-resolution mass spectrometry; HSQC, heteronuclear single-quantum coherence; NMR, nuclear magnetic resonance; PNPG, *p*-nitrophenolglucopyranoside; ROESY, rotating frame Overhauser effect spectroscopy; SPE, solid-phase extraction; *tt*, tube transfer

■ REFERENCES

(1) World Health Organization. Global status report on noncummunicable diseases 2010; available at www.who.int/nmh/publications/ncd_report2010 (accessed June 2013).

(2) Willett, W. C.; Sacks, F.; Trichopoulou, A.; Drescher, G.; Ferro-Luzzi, A.; Helsing, E.; Trichopoulos, D. Mediterranean diet pyramid: a cultural model for healthy eating. *Am. J. Clin. Nutr.* **1995**, *61*, 1402S−1406S.

(3) Bere, E.; Brug, J. Towards health-promoting and environmantally friendly regional diets − a Nordic example. *Public Health Nutr.* **2008**, *12*, 91−96.

(4) Välimäki, H.; Sørensen, L.; Dahlgren, M.; Malmin, R.; Redzepi, R.; Collin, R.; Lauterbach, E.; Hellstrøm, E.; Sigurdsson, F.; Fossdal, G., Örvarsson, H.; Björklund, M. Manifesto for the New Nordic Kitchen; www.clausmeyer.dk/en/the_new_nordic_cuisine_/manifesto_.html (accessed June 2013).

(5) Nordic Council of Ministers. The New Nordic Food programme: www.norden.org/en/nordic-council-of-ministers/council-of-ministers/council-of-ministers-for-fisheries-and-aquaculture-agriculture-food-and-forestry-mr-fjls/new-nordic-food (accessed June 2013).

(6) Mithril, C.; Dragsted, L. O.; Meyer, C.; Blauert, E.; Holt, M. K.; Astrup, A. Guidelines for the New Nordic Diet. *Public Health Nutr.* **2012**, *15*, 1941−1947.
(7) Micheelsen, A.; Holm, L.; O'Doherty Jensen, K. Consumer acceptance of the New Nordic Diet. An exploratory study. *Appetite* **2013**, *70*, 14−21.
(8) San Pellegrino World's 50 Best Restaurants; www.theworlds50best.com/awards/1-50-winners (accessed June 2013).
(9) Olsen, A.; Egeberg, R.; Halkjær, J.; Christensen, J.; Overvad, K.; Tjønneland, A. Healthy aspects of the Nordic diet are related to lower mortality. *J. Nutr.* **2011**, *141*, 639−644.
(10) Adamsson, V.; Reumark, A.; Fredriksson, I.-B.; Hammarstöm, E.; Vessby, B.; Johansson, G.; Risérus, U. Effects of a healthy Nordic diet on cardiovascular risk factors in hypercholesterolaemic subjects: a randomized controlled trial (NORDIET). *J. Intern. Med.* **2010**, *269*, 150−159.
(11) Espín, J. C.; García-Conesa, M. T.; Tomás-Barberán, F. A. Nutraceuticals: facts and fiction. *Phytochemistry* **2007**, *68*, 2986−3008.
(12) Chen, Z.-Y.; Jiao, R.; Ma, K. Y. Cholesterol-lowering nutraceuticals and functional foods. *J. Agric. Food Chem.* **2008**, *56*, 8761−8773.
(13) Vuorela, S.; Kreander, K.; Karonen, M.; Nieminen, R.; Hamalainen, M.; Galkin, A.; Laitinen, L.; Salminen, J.-P.; Moilanen, E.; Pihlaja, K.; Vuorela, H.; Vuorela, P.; Heinonen, M. Preclinical evaluation of rapeseed, raspberry, and pine bark phenolics for health related effects. *J. Agric. Food Chem.* **2005**, *53*, 5922−5931.
(14) Kool, J.; Giera, M.; Irth, H.; Niessen, W. M. A. Advances in mass spectrometry-based post-column bioaffinity profiling of mixtures. *Anal. Bioanal. Chem.* **2011**, *399*, 2655−2668.
(15) Shi, S.-Y.; Zhou, H.-H.; Zhang, Y.-P.; Jiang, X.-Y.; Chen, X.-Q.; Huang, K.-L. Coupling HPLC to on-line post column (bio)chemical assays for high-resolution screening of bioactive compounds from complex mixtures. *TrAC, Trends Anal. Chem.* **2009**, *28*, 865−877.
(16) Giera, M.; Irth, H. Simultaneuos screening and chemical characterization of bioactive compounds using LC-MS-based technologies (affinity chromatography). In *The Handbook of Environmental Chemistry: Effect Directed Analysis of Complex Environmental Contamination*; Brack, W., Ed.; Springer-Verlag: Berlin, Germany, 2011; pp 119−142.
(17) Giera, M.; Heus, F.; Janssen, L.; Kool, J.; Lingeman, H.; Irth, H. Microfractionation revisited: a 1536 well high resolution screening assay. *Anal. Chem.* **2009**, *81*, 5460−5466.
(18) Stærk, D.; Lambert, M.; Jaroszewski, J. W. HPLC-NMR techniques for plant extract analysis. In *Medicinal Plant Biotechnology. From Basic Research to Applications*; Kayser, O., Quax, W., Eds.; Wiley-VCH: Weinheim, Germany, 2006; pp 29−48.
(19) Seger, C.; Sturm, S. HPLC-SPE-NMR: a new hyphenation technique. *LC GC Eur.* **2007**, *11*, 587−597.
(20) Sandvoss, M.; Bardsley, B.; Beck, T. L.; Lee-Smith, E.; North, S. E.; Moore, P. J.; Edwards, A. J.; Smith, R. J. HPLC-SPE-NMR in pharmaceutical development: capabilities and applications. *Magn. Reson. Chem.* **2005**, *43*, 762−770.
(21) Staerk, D.; Kesting, J. R.; Sairafianpour, M.; Witt, M.; Asili, J.; Emami, S. A.; Jaroszewski, J. W. Accelerated dereplication of crude extracts using HPLC-PDA-MS-SPE-NMR: quinolinone alkaloids of *Haplophyllum acutifolium*. *Phytochemistry* **2009**, *70*, 1055−1061.
(22) Agnolet, S.; Jaroszewski, J. W.; Verpoorte, R.; Staerk, D. ^{1}H NMR-based metabolomics combined with HPLC-PDA-MS-SPE-NMR for investigation of standardized *Ginkgo biloba* preparations. *Metabolomics* **2010**, *6*, 292−302.
(23) Staerk, D.; Kesting, J. R.; Sairafianpour, M.; Witt, M.; Asili, J.; Emami, S. A.; Jaroszewski, J. W. Accelerated dereplication of crude extracts using HPLC-PDA-MS-SPE-NMR: quinolinone alkaloids of *Haplophyllum acutifolium*. *Phytochemistry* **2009**, *70*, 1055−1061.
(24) Sprogøe, K.; Stærk, D.; Jäger, A. K.; Adsersen, A.; Hansen, S. H.; Witt, M.; Landbo, A.-K. R.; Meyer, A. S.; Jaroszewski, J. W. Targeted natural product isolation guided by HPLC-SPE-NMR: constituents of *Hubertia* species. *J. Nat. Prod.* **2007**, *70*, 1472−1477.
(25) Sprogøe, K.; Stærk, D.; Ziegler, H. L.; Jensen, T. H.; Holm-Møller, S. B.; Jaroszewski, J. W. Combining HPLC-PDA-MS-SPE-NMR with circular dichroism for complete natural product characterization in crude extracts: levorotatory gossypol in *Thespesia danis*. *J. Nat. Prod.* **2008**, *71*, 516−519.
(26) Pukalskas, A.; van Beek, T. A.; de Waard, P. Development of a triple hyphenated HPLC-radical scavening detection-DAD-SPE-NMR system for the rapid identification of antioxidants in complex plant extracts. *J. Chromatogr., A* **2005**, *1074*, 81−88.
(27) Schmidt, J. S.; Lauridsen, M. B.; Dragsted, L. O.; Nielsen, J.; Staerk, D. Development of a bioassay-coupled HPLC-SPE-*tt*NMR platform for identification of α-glucosidase inhibitors in apple peel (*Malus* × *domestica* Borkh.). *Food Chem.* **2012**, *135*, 1692−1699.
(28) Grosso, C.; Jäger, A. K.; Staerk, D. Coupling of a high-resolution monoamine oxidase-A inhibitor assay and HPLC-SPE-NMR for advanced bioactivity-profiling of plant extracts. *Phytochem. Anal.* **2013**, *24*, 141−147.
(29) Agnolet, S.; Wiese, S.; Verpoorte, R.; Staerk, D. Comprehensive analysis of commercial willow bark extracts by new technology platform: combined use of metabolomics, high-perfomance liquid chromatography−solid-phase extraction−nuclear magnetic resonance spectroscopy and high-resolution radical scavenging assay. *J. Chromatogr., A* **2012**, *1262*, 130−137.
(30) Wubshet, S. G.; Nyberg, N. T.; Tejesvi, M. V.; Pirttilä, A. M.; Kajula, M.; Mattila, S.; Staerk, D. Targeting high-performance liquid chromatography-high-resolution mass spectrometry-solid-phase extraction-nuclear magnetic resonance analysis with high-resolution radical scavenging profiles − bioactive secondary metabolites from the endophytic fungus *Penicillium namyslowskii*. *J. Chromatogr., A* **2013**, *1302*, 34−39.
(31) Wiese, S.; Wubshet, S. G.; Nielsen, J.; Staerk, D. Coupling HPLC-SPE-NMR with a microplate-based high-resolution antioxidant assay for efficient analysis of antioxidants in food − validation and proof-of-concept study with caper buds. *Food Chem.* **2013**, *141*, 4010−4018.
(32) Leonti, M.; Nebel, S.; Rivera, D.; Heinrich, M. Wild gathered food plants in the European mediterranean: a comparative analysis. *Econ. Bot.* **2006**, *60*, 130−142.
(33) Jahangir, M.; Kim, H. K.; Choi, Y. H.; Verpoorte, R. Health-affecting compounds in Brassicaceae. *Comp. Rev. Food Sci. Food Saf.* **2009**, *8*, 31−43.
(34) Albayrak, S.; Aksoy, A.; Sagdic, O.; Hamzaoglu, E. Compositions, antioxidant and antimicrobial activities of *Helichrysum* (Asteraceae) species collected from Turkey. *Food Chem.* **2010**, *119*, 114−122.
(35) Re, R.; Pellegrini, N.; Proteggente, A.; Pannala, A.; Yang, M.; Rice-Evans, C. Antioxidant activity applying an improved ABTS radical cation decolorization assay. *Free Radical Biol. Med.* **1999**, *26*, 1231−1237.
(36) Schmidt, B.; Jaroszewski, J. W.; Bro, R.; Witt, M.; Stærk, D. Combining PARAFAC analysis of HPLC-PDA profiles and structural characterization using HPLC-PDA-SPE-NMR-MS experiments: commercial preparations of St. John's wort. *Anal. Chem.* **2008**, *80*, 1978−1987.
(37) Gao, H.; Huang, Y.-N.; Gao, B.; Xu, P.-Y.; Inagaki, C.; Kawabata, J. α-Glucosidase inhibitory effect by the flower buds of *Tussilago farfara* L. *Food Chem.* **2008**, *106*, 1195−1201.
(38) Ha, T. J.; Lee, J. H.; Lee, M. H.; Lee, B. W.; Kwon, H. S.; Park, C. H.; Shim, K. B.; Kim, H. T.; Baek, I. Y.; Jang, D. S. Isolation and identification of phenolic compounds from the seeds of *Perilla frutescens* (L.) and their inhibitory activities against α-glucosidase and aldose reductase. *Food Chem.* **2012**, *135*, 1397−1403.
(39) Baris, O.; Karadayi, M.; Yanmis, D.; Guvenalp, Z.; Bal, T.; Gulluce, M. Isolation of 3 flavonoids from *Mentha longifolia* (L.) Hudson subsp. *longifolia* and determination of their genotoxic potentials by using the *E. coli* WP2 test system. *J. Food Sci.* **2011**, *76*, 212−217.

(40) Kroll, U.; Reif, K.; Lederer, I.; Förster, G.; Zapp, J. Kaempferol-3,4′-di-*O*-*β*-glucopyranoside-7-*O*-*α*-rhamnopyranoside as a new flavonoid from *Iberis amara* L. *Pharmazie* **2009**, *64*, 142−144.
(41) Markham, K. R.; Hammett, K. R. W.; Ofman, D. J. Floral pigmentation in 2 yellow-flowered *Lathyrus* species and their hybrid. *Phytochemistry* **1992**, *31*, 549−554.
(42) Mulinacci, N.; Vincieri, A. B.; Baldi, A.; Bambagiotti-Alberti, M.; Sendl, A.; Wagner, H. Flavonol glycosides from *Sedum telephium* subspecies *maximum* leaves. *Phytochemistry* **1995**, *38*, 531−533.
(43) Miyake, Y.; Mochizuki, M.; Okada, M.; Hiramitsu, M.; Morimitsu, Y.; Osawa, T. Isolation of antioxidative phenolic glucosides from lemon juice and their suppressive effect on the expression of blood adhesion molecules. *Biosci., Biotechnol., Biochem.* **2007**, *71*, 1911−1919.
(44) Baumert, A.; Milkowski, C.; Schmidt, J.; Nimtz, M.; Wray, V.; Strack, D. Formation of a complex pattern of sinapate esters in *Brassica napus* seeds, catalyzed by enzymes of a serine carboxypeptidase-like acyltransferase family. *Phytochemistry* **2005**, *66*, 1334−1345.
(45) Gerothanassis, I. P.; Exarchou, V.; Lagouri, V.; Troganis, A.; Tsimidou, M.; Boskou, A. Methodology for identification of phenolic acids in complex phenolic mixtures by high-resolution two-dimensional nuclear magnetic resonance. Application to methanolic extracts of two oregano species. *J. Agric. Food Chem.* **1998**, *46*, 4185−4192.
(46) Foti, M. C. Antioxidant properties of phenols. *J. Pharm. Pharmacol.* **2007**, *59*, 1673−1685.
(47) Walle, T.; Browning, A. M.; Steed, L. L.; Reed, S. G.; Walle, U. K. Flavonoid glucosides are hydrolyzed and thus activated in the oral cavity in humans. *J. Nutr.* **2005**, *135*, 48−52.
(48) Bokkenheuser, V. D.; Shackleton, C. H. L.; Winter, J. Hydrolysis of dietary flavonoid glycosides by strains of intestinal bacteroides from humans. *Biochem. J.* **1987**, *248*, 953−956.
(49) Wang, H.; Du, Y. J.; Song, H. C. *α*-Glucosidase and *α*-amylase inhibitory activities of guava leaves. *Food Chem.* **2010**, *123*, 6−13.
(50) Kim, J. S.; Kwon, C. S.; Son, K. H. Inhibition of *α*-glucosidase and amylase by luteolin, a flavonoid. *Biosci., Biotechnol., Biochem.* **2000**, *64*, 2458−2461.